Structural Eng. / Earthquake Eng. Vol. 3. No. 2, 447s-456s. October 1986
Japan Society of Civil Engineers (Proc. of JSCE No. 374 / I-6)

DYNAMICS OF A LIQUID STORAGE TANK PLACED ON AN ELASTIC FOUNDATION

By Narioki AKIYAMA, Hiroki YAMAGUCHI** and Yukio ENYA****

The dynamic behavior of a liquid storage tank placed on an elastic foundation is studied analytically and experimentally. The coupled method of FEM-BEM is firstly developed for the dynamic analysis of the fluid-structure-foundation coupled system and the accuracy of the method is demonstrated for the sloshing, ovaling and rocking oscillations. The results of the numerical analysis are compared with the results of experiments conducted with a flexible cylindrical tank placed on an elastic foundation. The effects of the flexibility of the foundation are finally investigated on the dynamic characteristics of coupled motion of the tank.

Keyword : liquid storage tank, elastic foundation, coupled oscillation, seismic design

1. INTRODUCTION

Lately, by the large demand for energy, huge-scaled tanks containing inflammable liquid, such as petroleum, LNG, LPG and so forth, have been progressively constructed throughout this conutry, raising the problem of rational evaluation of aseismic safety. We shall not mention the importance of aseismic design of tank of this type and the research trend of the relevant problem thoroughly discussed in Refs. 1) and 2), however, one thing must be said that coupling oscillation with surrounding ground is one of the most crucial problem[2]. To be more specific, huge circular cylindrical tanks are most commonly built on relatively soft foundation, and so constitutes the complicated vibrating system of Liquid-Tank-Foundation. Though various approaches[3)~7)] have been attempted both theoretically and experimentally so far, the dynamic characteristics of the above system, especially the foundation effect, have not been identified each other and remain unsolved from the standpoint of these approaches.

The present paper proposes the analysis method for coupling oscillation of Liquid-Tank-Foundation system, combining the finite element method (FEM) and the boundary element method (BEM). Verifying the accuracy in numerical analysis, an attempt of understanding the dynamic characteristics of the above system is undertaken by comparing test and calculated results by the proposed method.

2. FEM-BEM COUPLED ANALYSIS

(1) Analytical model

The liquid storage tank placed on an elastic foundation is the fluid-structure-foundation coupled

* Member of JSCE, Dr. Eng., Prof. of Foundation Eng., Saitama Univ. (255 Shimo-Ohkubo, Urawa, Saitama).
** Member of JSCE, Dr. Eng., Asst. Prof. of Foundation Eng., Saitama Univ..
*** Student Member of JSCE, Graduate Student, Saitama Univ..

oscillating system which is composed of four oscillating elements ; the contained liquid, the tank wall, the bottom plate and the elastic foundation. In the present paper, the so-called FEM-BEM coupled analysis is adopted. That is, the contained liquid is discretized by BEM while the tank wall, the bottom plate and the elastic foundation are discretized by FEM.

The assumptions introduced in the analysis are follows :

a) The contained liquid is inviscid, incompressible and in an irrotational motion. The flow is then taken to be potential. The motion at the free surface is small enough to apply the theory of small-amplitude wave.

b) The thin shell theory is applicable for the tank wall.

c) The stretching of the bottom plate is neglected but the bending of the plate is only considered.

d) The tank wall and the bottom plate are connected rigidly. The deflection angle is continuous at the connection.

e) The foundation is isotropic and elastic.

(2) Element matrices for each oscillating element

A cylindrical co-ordinate system is used and the radial, circumferential and axial co-ordinates are denoted by r, θ and z, respectively. Every unknown variables are expanded in Fourier series with respect to the circumferential co-ordinate θ, according to the axisymmetry of the problem. The characteristic element matrices, such as the stiffness matrix etc., are then obtained independently for each Fourier coefficient under the assumption of linear analysis.

a) Contained liquid——potential flow boundary element[8),9)]

The velocity potential of the contained fluid, $\phi(r, \theta, z, t)$, satisfies the Laplace's equation

$$\nabla^2\phi=0 \quad \cdots\cdots (1)$$

in the domain Ω (Fig. 1) according to the assumption a). This Laplace's equation is transformed into an integral equation on the boundary Γ using Green's theorem. Expanding the velocity potential into a Fourier series and using the orthogonality of trigonometric function, one can obtain the following integral equation.

$$\sum_{m=0}^{\infty} \pi r_i \phi_m(r_i, z_i)+\int_\Gamma \sum_{m=0}^{\infty} \phi_m \cos m\theta \cdot q^* d\Gamma=\int_\Gamma \sum_{m=0}^{\infty} q_m \cos m\theta \cdot \phi^* d\Gamma \quad \cdots\cdots (2)$$

where ϕ_m and q_m are the m-th Fourier coefficients of velocity potential and flux on the boundary Γ, respectively. The flux q is defined as the first derivative of the velocity potential ϕ with respect to the external normal n at a point on the boundary Γ ; $q=\partial\phi/\partial n$.

ϕ^* and q^* in Eq. (2) are the so-called fundamental solution which are the particular solution of the Laplace's equation due to the source potential, $\sum_{k=0}^{\infty} \cos k\varphi / r_i$, distributed on a circular arc at $r=r_i$, $z=z_i$ (Fig. 2). It can be considered that there is the concentrated potential, $(\sum_{k=0}^{\infty} \cos k\varphi / r_i) \cdot r_i d\varphi$, at the source point $P(r_i, \varphi, z_i)$. The increment of potential at the arbitrary receiving point $Q(r, \theta, z)$ due to this concentrated potential is described as

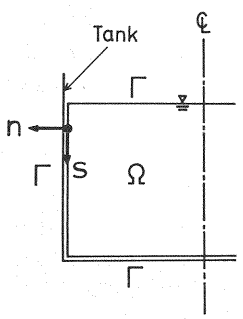

Fig. 1 Potential problem for the liquid content.

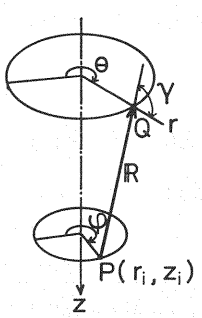

Fig. 2 Source point and receiving point.

$$d\phi^*=-1/4\pi R\cdot\sum_{k=0}^{\infty}\cos k(\theta-\alpha)\cdot d\alpha \quad (3\cdot a)$$

in which

$$R^2=r^2+r_i^2-2rr_i\cos\alpha+(z-z_i)^2 \quad (3\cdot b)$$

$$\alpha=\theta-\varphi \quad (3\cdot c)$$

The fundamental solutions ϕ^*, q^* are then obtained by the integration of Eq. (3·a).

$$\phi^*=\oint d\phi^*=\sum_{k=0}^{\infty}(\phi_k^*\cos k\theta+\bar{\phi}_k^*\sin k\theta) \quad (4\cdot a)$$

$$q^*=\oint \partial\cdot d\phi^*/\partial n=\sum_{k=0}^{\infty}(q_k^*\cos k\theta+\bar{q}_k^*\sin k\theta) \quad (4\cdot b)$$

where

$$\phi_k^*=\int_0^{2\pi}\frac{\cos k\alpha}{4\pi R}d\alpha\ ,\quad \bar{\phi}_k^*=\int_0^{2\pi}\frac{\sin k\alpha}{4\pi R}d\alpha \quad (5\cdot a, b)$$

$$q_k^*=-\int_0^{2\pi}\frac{\cos\gamma\cdot\cos k\alpha}{4\pi R^2}d\alpha\ ,\quad \bar{q}_k^*=-\int_0^{2\pi}\frac{\cos\gamma\cdot\sin k\alpha}{4\pi R^2}d\alpha \quad (5\cdot c, d)$$

In Eqs. (5·c, d), γ is the angle between the external normal of the boundary at Q and the relative position vector of Q with respect to P.

Substituting Eqs. (4·a, b) into Eq. (2) and introducing co-ordinate s defined by the length along the meridian on the boundary, the following equation is derived.

$$c_i\phi_k(r_i,z_i)+\int_\Gamma(\phi_k q_k^*-q_k\phi_k^*)\,r(s)\cdot ds=0 \quad (6)$$

where c_i is a coefficient determined by the condition of the boundary at the source point. In the case of smooth boundary, c_i equals to 1/2.

The boundary Γ in the boundary integral equation (6) is subdivided into finite elements and the distribution of velocity potential in each element is assumed to be linear. The final matrix form of equation is then obtained for the nodal velocity-potential ϕ_k and the nodal flux q_k;

$$\{\phi_k\}=[C_k]\{q_k\} \quad (7)$$

where $[C_k]$ is a coefficient matrix corresponding to the Fourier number k.

b) Tank wall——cylindrical shell element

The axisymmetric thin shell element[10] is adopted for tank wall. The tank wall is subdivided into several circular ring elements shown in Fig. 3 and the vertical, circumferential, radial components of displacement, u_s, v_s, w_s, and the first derivative of w_s with respect to z, β_s, are considered as four components of the nodal displacement vector.

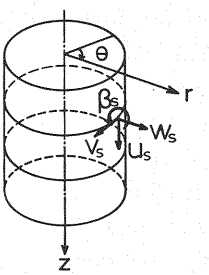

Fig. 3 Cylindrical shell element.

The usual cylindrical-shell-element corresponding to Love's Theory is utilized in the present paper but the effect of the initial circumferential stress $\sigma_{\theta 0}$ due to the hydrostatic pressure of contained liquid are evaluated in the stiffness matrix. The initial stress $\sigma_{\theta 0}$ is written as

$$\sigma_{\theta 0}=\rho g\{z-(L-H)\}\,a/t \qquad z\geq L-H \quad (8)$$

where ρ is the liquid density, g is the gravitational acceleration, L is the height of take wall, H is the depth of contained liquid, a and t are the radius and thickness of the cylindrical shell. The effect of initial stress in the stiffness matrix can be evaluated by considering the potential energy due to the initial stress $\sigma_{\theta 0}$ with the nonlinear strain-displacement relation.

After the element stiffness matrix is obtained, the stiffness matrix for the tank wall is derived. As for the mass matrix, the consistent mass matrix[11] are utilized as is usual in the finite element analysis.

c) Bottom plate——axisymmetric plate element

The bottem plate is modeled by the axisymmetric plate element[10] and is subdivided into a circular plate element and several ring plate elements shown in Fig. 4. The variables at each node are the vertical

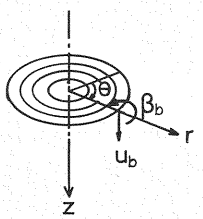

Fig. 4 Axisymmetric plate element.

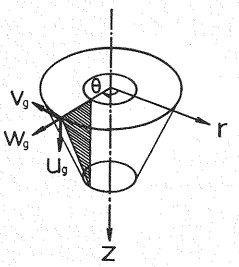

Fig. 5 3-nodes axisymmetric body element.

deflection u_b and the angle of deflection β_b. The shape function of out-of-plane displacement u_b then should be a 3rd order polynomial for the ring plate element. The following higher-order shape function, however, is used for the circular plate element because of the singularity at the center; $r=0$.

$$u_{bk}(r)=\alpha_{1k}r^k+\alpha_{2k}r^{k+2} \quad (9)$$

in which k is the Fourier number.

The potential energy for one element gives the element stiffness matrix of axisymmetric plate and the whole stiffness matrix of the bottom plate will be derived. The consistent mass matrix is adopted as was used for the tank wall.

d) Elastic foundation——3 nodes axisymmetric body element[10]

The elastic foundation is subdivided into several axisymmetric body elements with triangular cross sections and the nodal displacement vector is composed of the vertical, circumferential and radial components of displacement, u_g, v_g and w_g (Fig. 5). The stiffness and mass matrices for the elastic foundation is obtained using the ordinary way of FEM.

(3) Equation of motion for Liquid-Tank-Foundation system

The characteristic matrices for each vibrating element; contained liquid, tank shell, bottom plate and foundation, are superposed in order to derive the equation of motion in the global co-ordinate system using the boundary condition.

a) Equation of motion for Tank-Foundation system

As for the coupled equation of motion for the tank-foundation system without the vibrating element of liquid, the direct stiffness method[12] is applicable because the stiffness and mass matrices of tank and foundation have been obtained by FEM. The horizontal displacement of the bottom plate, however, is introduced as a rigid-body movement in order to analyze the rocking oscillation which is one of the most important phenomenon of the tank placed on an elastic foundation. Specifically speaking, the radial and circumferential components of the horizontal rigid-body-motion of the bottom plate are superimposed only to the 1st Fourier coefficients of foundation displacements.

It is assumed in the present paper that there is no sliding nor separation between the bottom plate and the foundation.

b) Superposition of the liquid element matrix

It is introduced as a boundary condition between the contained liquid and the tank that the deformation velocity of tank equals to the flow velocity of contained liquid. According to this boundary condition, the following equation can be derived from Eq. (7).

$$\{p\}=-\rho[C]\{\ddot{u}\} \quad (10)$$

where $\{p\}$ is the hydrodynamic pressure vector acting on the tank, $\{u\}$ is the displacement vector of the tank in the normal direction and a superposed dot represents a time derivative. Transforming the dynamic pressure (10) to the equivalent nodal force using the principle of virtual work, a part of the liquid element matrix $[C]$ is superposed into the mass matrix of tank as additional masses.

As for the remaining part of $[C]$ which corresponds to the free surface of contained liquid, the theory of

small amplitude wave[13] ;

$$\rho\dot{\phi}+\rho g\zeta=0 \quad \cdots\cdots (11)$$

is assumed as is mentioned in 2. (1) and Eq. (7) is transformed into the equation of motion for the vertical displacement vector of fluid at the free surface, $\{\zeta\}$, as

$$\rho[C]\{\ddot{\zeta}\}+\rho g\{\zeta\}=\{0\} \quad \cdots\cdots (12)$$

Following the procedure described above, the coupled equation of motion for the whole system of Liquid-Tank-Foundation is finally obtained in the matrix form ;

$$[M]\{\ddot{x}\}+[K]\{x\}=\{0\} \quad \cdots\cdots (13)$$

where $\{x\}$ is the total displacement vector consisting of the displacements of tank, liquid at the free surface and foundation. $[M]$ and $[K]$ are the mass and stiffness matrices for the total system.

(4) Stationary response to horizontal ground motion

The analysis on the stationary response of the liquid-tank-foundation system due to a simple harmonic ground motion can be done by means of applying the modal analysis after the natural oscillations are obtained from Eq. (13). The horizontal ground motion has no excitation for the higher Fourier numbers other than for the first one ; $k=1$. The responses to the higher Fourier components of excitation, however, are analyzed in the present paper according to demand, because it was reported in the experimental studies[14),15)] that there existed several percents of input excitation even for the higher Fourier numbers according to the initial imperfections of tank wall.

3. ACCURACY OF NUMERICAL SOLUTIONS

Behaviors of numerical solutions by FEM-BEM coupled method developed in the last chapter are very complicated due to the liquid-tank-foundation coupling system. For this reason, both theoretical and programming mistakes are liable to be committed and difficult to be detected, which leads to the indispensable confirmation of numerical solution accuracy.

(1) Solution accuracy of sloshing motion

Sloshing motion comprising only fliud motion is subject to examination for the case of rigid tank (25 cm in diameter, 40 cm high, 12.5 cm in water depth) and rigid foundation, by comparing results between by the potential theory[16)] and the present method. Natural frequencies given in Table 1 show the good agreement within 2 % up to 3rd mode. Comparisons are also given in Fig. 6 around the fundamental resonance for

Table 1 Natural frequencies of sloshing mode.

Mode	Vel. potential theory (Hz)	The proposed FEM-BEM (Hz)
1	1.86	1.87
2	3.25	3.21
3	4.12	4.07
4	4.82	4.81
5	5.44	5.41
6	5.98	5.90

Table 2 Natural frequencies of ovaling mode.

	Fourier number	Mode number	Proposed FEM-BEM (Hz)	By Haroun[17)] (Hz)	By Zui[15)] (Hz)
Broad tank	1	1	6.26	6.18	6.17
		2	11.00	11.28	11.13
	5	1	3.04	2.76	2.79
		2	8.37	8.37	8.14
Tall tank	1	1	5.79	5.31	5.36
		2	14.80	15.64	15.71
	5	1	2.17	—	2.05
		2	4.41	—	4.37

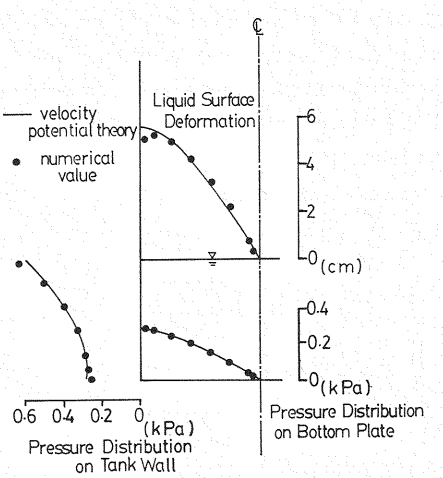

Fig. 6 Sloshing response of the tank.

sloshing height and hydrodynamic pressures against tank wall and bottom plate, showing the good agreement as well.

(2) Solution accuracy of ovaling motion

For ovaling motion comprising the coupling motion of tank and fluid, comparisons are made on the numerical results with those in Refs. 15) and 17), and given in Table 2. This table again shows the reasonably good agreement for broad tank and tall tank as well.

(3) Solution accuracy of rocking motion

For rocking motion comprising the coupling motion of tank and foundation, solution accuracies are verified by applying the proposed method to the test model in Ref. 7). The tank model employed is of acrylic, 63.5 cm high, 40 cm in diameter, 1 cm thick and has the 3.5 cm thick bottom plate. Elastic foundation is made of 7 cm thick plastigel (density : 0.118×10^{-5} kg/cm^3, longitudinal elastic modulus : 46.0 KPa, Poisson's ratio : 0.47).

Hydrodynamic pressure response curves are given in Fig. 7 for rigid tank at the bottom point 2 cm inward from the tank wall and comparisons are made versus damping coefficient h's. W_i in this figure corresponds to the i-th sloshing mode and G_j to the j-th mode of foundation motion. All the resonance peaks except G_1 vanish when damping coefficient h increases. G_1 mode is given in Fig. 8 corresponding to rocking motion due to shear mode of foundation motion. The excessive shear mode is caused by the very soft and bounded foundation. The slight difference in natural frequency (0.5 Hz) is supposedly due to difficulty in exact evaluation for soft material[7]. On the other hand, response values, though depending on the uncertain factor h, can be interrelated between the numerical calculation and the test.

4. COUPLED RESPONSE OF FLEXIBLE TANK ON ELASTIC FOUNDATION

(1) Vibration test with a flexible tank model

In order to investigate the coupled oscillation between the liquid storage tank and the foundation, a vibration test has been made by using a flexible tank model and an elastic foundation model. The test equipment is shown in Fig. 9.

We used the shaking table (MHI, NH-8854), in the Ohkubo Experiment Station of Water Resources Development Public Corporation. The cylindrical tank model, which was tested experimentally, is 50 cm in inside diameter and 50 cm in height. The thickness of tank wall is 0.08 cm and the thickness of bottom plate is 0.10 cm. The tank material is vinyle choride ; the Young's modulus is 3.2 GPa, the Possion's ratio is 0.3 and the density is 0.144×10^{-5} kg/cm^3. City water was used for the contained liquid as a matter of convenience and the water depth is 30 cm. The elastic foundation model is a rectangxlar prism with a base of 120 cm×120 cm and a height of 7 cm. The model was made of plastigel and was same as the one used in the rigid-tank experiment[7] mentioned in 3. (3).

The measurement items and the measuring method are as follows :

a) The acceleration of the shaking table is measured by an accelerometer in order to check the input acceleration.

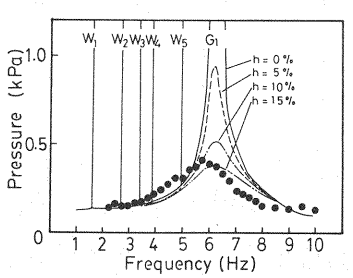

Fig. 7 Frequency response of hydrodynamic pressure.

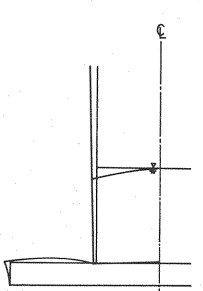

Fig. 8 Rocking mode G_1.

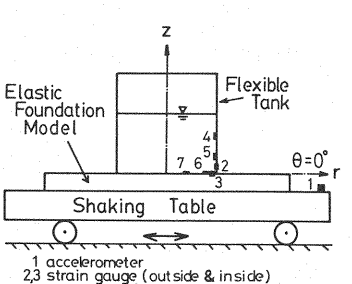

Fig. 9 Test equipment.

b) In order to measure hydrodynamic pressures, four pressure gauges were located at two points on the tank wall ; $\theta=0^\circ$, $z=10$ cm and 20 cm, and at two points on the bottom plate ; $\theta=0^\circ$, $r=10$ cm and 20 cm.

c) Strain gauges were applied to the inner and outer tank surface in order to investigate the deformation of tank. The measuring points were on the wall ; $\theta=0^\circ$, $z=5$ cm, and on the plate ; $\theta=0^\circ$, $r=20$ cm.

The elastic foundation model was fixed on the shaking table and the flexible tank model was placed on the foundation model without anchor. A horizontal simple harmonic excitation of shaking table was applied under acceleration control. The frequency range of input excitation was between 2 Hz and 20 Hz, and the interval of each excitation was 0.5 Hz but was 0.25 Hz in the region of the resonance frequency. The input acceleration was 0.075 g.

(2) Comparison of test and calculated results and discussion

Frequency response curves of hydrodynamic pressure against tank wall ($z=20$ cm, $\theta=0^\circ$) and bottom plate ($r=20$ cm, $\theta=0^\circ$) are given in Figs. 10 and 11, respectively. Here, ● means the measured value and curves are parametrically constructed by damping coefficient h and Fourier number $k=1$. W_i and G_j's in these figures mean i-th sloshing mode and j-th mode of foundation motion, respectively, identified by calculated mode shapes.

a) Sloshing response

As seen from Figs. 10 and 11, test results do not show the significant hydrodynamic response for higher sloshing modes, successfully explained by numerical results. Numerical results also has shown that sloshing response of the flexible tank on deformable ground agrees with that of rigid tank on rigid ground, derived from velocity potential theory. The comparison of natural frequency is shown in Table 3. It is also confirmed that flexibilities of tank and ground have nothing to do with the sloshing phenomena.

b) Rocking response

Test results show two resonance peaks around the frequencies of 6.5 Hz and 16.0 Hz. Numerical results

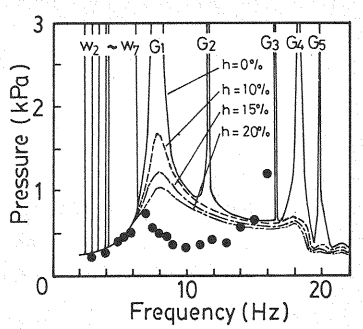

Fig. 10 Frequency response of hydrodynamic pressure ——tank wall.

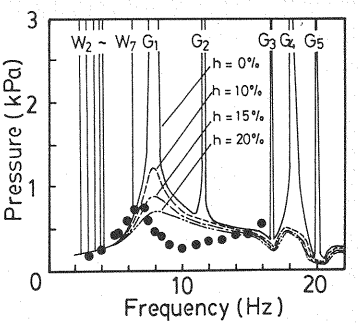

Fig. 11 Frequency response of hydrodynamic pressure ——bottom plate.

Table 3 Comparison of natural frequencies for sloshing modes.

Mode	Rigid tank & foundation(Hz)	Flex. tank & elastic f.(Hz)
1	1.35	1.35
2	2.30	2.29
3	2.91	2.93
4	3.41	3.42
5	3.84	3.83
6	4.23	4.13

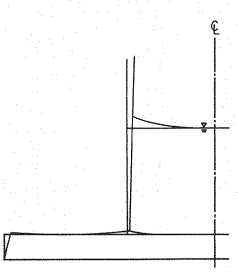

Fig. 12 G_1-mode.

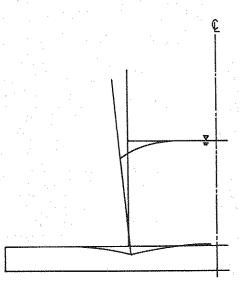

Fig. 13 Rocking mode G_4.

show that in case of $h=0$, there appear resonance peaks corresponding to W_2-W_7 and G_1-G_5, but all the peaks except G_1 and G_4 supposedly vanish as h increases, eventually corresponding to the two resonance peaks observed in the test.

G_1 and G_4 modes are given in Figs. 12 and 13 by free oscillation analysis. G_1 is one and the same mode as G_1 for the rigid tank, corresponding to the one due to shear mode of ground motion, while G_4 clearly corresponds to the rocking mode of tank. Slight deviation of national frequency between test and calculation is much the same as in the case of rigid tank and supposedly due to the estimation error of elastic constants of the ground material.

The hydrodynamic pressure distributions around the resonance peaks are given in Figs. 14 and 15. Measured values ● and ▲ mean hydrodynamic response values against tank wall and bottom plate, respectively. Solid lines mean calculated results, corresponding to the case of $k=1$, $h=20$ %. These results are obtained consideing the deviation in natural frequencies mentioned above. That is, the frequencies of excitation are 7.0 Hz, 16.0 Hz for the experiment and 8.4 Hz, 18.0 Hz for the analysis. A good agreement is observed in Fig. 14 between test and numerical analysis results for G_1 mode. For G_4 mode in Fig. 15, a good agreement is also shown for bottom plate, but not for tank wall considering that calculated results come to only half measured values. This deviation is supposedly due to the effect of 3rd mode ($k=3$) in ovaling response explained later.

c) Ovaling response

Strain measurements are taken both on inner and outer surfaces in the test, so that frequency responses of bending and membrane stresses can be obtained. Fig. 16 shows the one for the measuring point on the tank wall. In the figure, θ and z direction mean the circumferential and vertical components of stress on the wall. The examination of this frequency response tells that bending stress is far greater than membrane stress in the frequency band corresponding to G_1 mode, while in G_4 mode stress ratio (bending stress/membrane stress) come to around unity, due to the increase in membrane stress caused by increasing hydrodynamic pressure toward the higher frequency band.

Though the ovaling effect is expected on the increasing hydrodynamic pressure along the upper part of tank wall, ovaling mode frequency for the 1 st mode of tank wall ($k=1$) reaches around 250 Hz, so this ovaling mode impossibly exerts the effect on the increase in hydodynamic pressure. Zui et al.[5] point out that the ovaling vibration mode for $k=3$ is the most significantly induced by inherent initial imperfections under horizontal excitation (corresponding to the 1st Fourier number).

The frequency response of the hydrodynamic pressure for $k=3$ against tank wall is given in Fig. 17. For simplicity, the input is assumed 10 % that for the case $k=1$. This figure shows that two ovaling modes S_1 and S_2 appear at the frequency corresponding to G_4 mode, bringing about the increased membrane stress. Fig. 18 shows the calculated S_2-mode shape quite same as the S_1-mode shape. The fact that the foundation

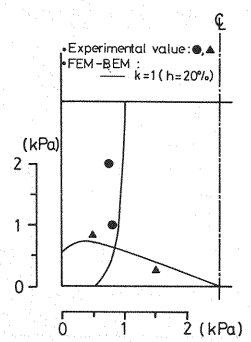

Fig. 14 Pressure distribution—G_1-response.

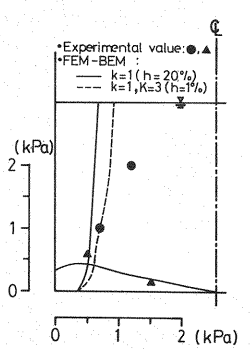

Fig. 15 Pressure distribution—G_4-response.

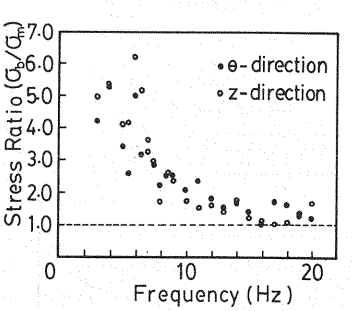

Fig. 16 Frequency response of stress ratio.

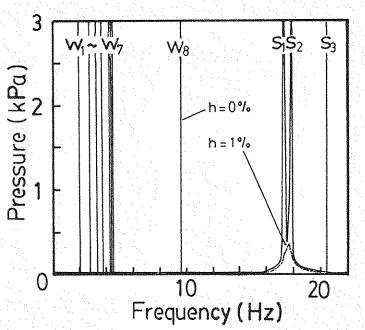

Fig. 17 Frequency response of hydrodynamic pressure (k=3).

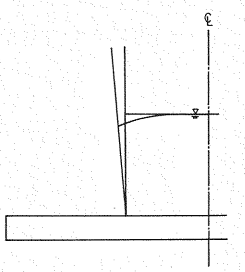

Fig. 18 Ovaling mode S_2 (k=3).

does not move in case of S_1 and S_2 modes makes us assume the low damping constant (h=1%) in the calculation.

Numerical results obtained by superposition of the hydrodynamic pressure for S_2 mode to that for G_4 mode show the resonable agreement with the measured results (the broken line in Fig. 15), showing the significance of S_2 mode. The calculation also shows that the natural frequency of S_2 mode for the flexible foundation is 17.7 Hz, while 73.7 Hz for the rigid foundation, telling that the frequency of ovaling vibration is greatly reduced by supporting condition and possibly falls within the resonance frequency band for G_4 mode of rocking motion.

The resonance peak around 16 Hz in our test is supposed to be the coupling response between G_4 mode of rocking mode and S_2 mode of ovaling motion, and also the cause of the increased hydordynamic pressure against tank wall. This coupling vibration accelerates overturning moment involving the uplift of tank. Due consideration must be given to the reduction in the natural frequency of ovaling vibration of flexible tank on elastic foundation.

5. CONCLUSION

The analysis is made on the dynamic characteristics of circular cylindrical flexible tank on elastic foundation theoretically and experimentally as well, with special emphasis on the flexibility of foundation. The validity of the proposed method, applying BEM to the contained fluid and FEM to the elastic foundation, is confirmed by the accuracy of numerical solutions under various conditions. The test employing the flexible tank model with water content on the deformable foundation under horizontal exctation is analyzed and examined by the proposed method from the aspect of the hydrodynamic pressure against tank wall and stress values.

The following dynamic characteristics of liquid storage tank on elastic foundation are made clear :

1) As one of the most important vibration mode for the tank on elastic forndation, there exists a well-defined rocking motion (k=1) between sloshing mode at lower frequency and ovaling motion at higher frequency. In this motion hydrodynamic pressure against tank wall is exaggerated.
2) The natural frequency of ovaling motion for elastic foundation is possibly reduced to almost the same frequency for rocking motion.
3) As natural frequencies of rocking and ovaling oscillation are located somewhat closely each other, the responses for these motions are superimposed, among other thing, exaggerating the hydrodynamic pressure against the upper part of tank wall. This phenomenon leads to raise the possibility of uplift of tank.
4) Flexibilities of tank and foundation have nothing to do with the sloshing motion.

ACKNOWLEDGEMENT

We owe the test in the present paper to Messrs. Ohashi and Shino (former students of Saitama

University). Cordial thanks are also extended to Messrs. Hosoya, Ichikawa, Shiraishi, Kobayashi, Sasaki (former students of Saitama University) and Abe (former graduate student of Saitama University) for their assistance for developing computer program.

REFERENCES

1) Shimizu, N. : Research trend of aseismic design of liquid storage tanks, Proc. of JSME, Vol. 49, No. 438, pp. 145～153, Feb. 1983 (in Japanese).
2) Sakai, F. : Studies on seismic design of liquid storage tanks——present and furture, Proc. of JSCE, Structural Eng./Earthquake Eng. Vol. 2, No. 2, pp. 1～11, Oct. 1985 (in Japanese).
3) Investigation Report on the safety of the integrated system of tank-foundation, Energy Committee JSCE, 1982 (in Japanese).
4) Oaku, S. and Kokusho, T. : Axisymmetric coupling vibration analysis of liquid-tank-foundation system, The 15 Symp. on Earthquake Eng. Research, JSCE, pp. 217～220, July 1979 (in Japanese).
5) Sakai, F. and Ogawa, H. : Bulging vibration of circular cylindrical liquid storage tank considering rocking motion, Proc. 6 th Nat. Symp. on Earthquake Eng., pp. 1329～1335, Dec. 1982 (in Japanese).
6) Umebayashi, S. et al. : Radiation damping of cylindrical liquid storage tank resting on semi-infinite elastic body, JHPI Vol. 21, No. 1, pp. 48～55, Jan. 1983 (in Japanese).
7) Ikeda, S. et al. : Research on the lateral and rocking vibration of a cylindrical tank placed on a horizontally oscillating elastic layer, Report of Dept. Found. Eng. and Const. End., Saitama Univ., Vol. 12, pp. 135～165, 1982 (in Japanese).
8) Brebbia, C. A. ed. : PROGRESS IN BOUNDARY ELEMENT METHODS, VOL. 2, Pentech Press Ltd., 1983.
9) Tanaka, M. and Tanaka, K. : BOUNDARY ELEMENT METHOD-FUNDAMENTAL AND APPLICATION, Maruzen, 1982 (in Japanese).
10) Washizu, K. et al. ed. : HANDBOOK OF FINITE ELEMENT METHOD, VOL. I, Baifukan, 1983 (in Japanese).
11) Washizu, K. et al. ed. : HANDBOOK OF FINITE ELEMENT METHOD, VOL. II, Baifukan, 1983 (in Japanese).
12) Desai, C. S. and Abel, J. F. : INTRODUCTION TO THE FINITE ELEMENT METHOD, Van Nostrand Reinhold Co., 1972.
13) Hino, M. : FLUID DYNAMICS, Asakura-shoten, 1974 (in Japanese).
14) Clough, R. W. et al. : Experimental seismic study of cylindrical tanks, Proc. of ASCE, Vol. 105, No. ST 12, pp. 2565～2590, Dec. 1979.
15) Zui, H. and Shinke, T. : Seismic response analysis of cylindrical tanks with initial imperfections, Proc. of JSCE, Structural Eng./Earthquake Eng. Vol. 1, No. 2, pp. 207～216, Oct. 1984 (in Japanese).
16) Ikeda, S. et al. : Study on the sloshing of liquid contained in circular tank, Proc. of JSCE, Vol. 290, pp. 53～65, Oct. 1979 (in Japanese).
17) Haroun, M. A. : Vibration study and tests of liquid storage tanks, Earthquake Eng. and Struct. Dynamics, Vol. 11, pp. 179～206, 1983.

(Received April 7 1986)